

LHC Phenomenology of SO(10) Models with Yukawa Unification II

Archana Anandakrishnan[†], B. Charles Bryant[†], and Stuart Raby[†]

[†]*Department of Physics, The Ohio State University,
191 W. Woodruff Ave, Columbus, OH 43210, USA*

November 15, 2018

Abstract

In this paper we study Yukawa-unified SO(10) SUSY GUTs with two types of SO(10) boundary conditions: (i) universal gaugino masses and (ii) non-universal gaugino masses with *effective “mirage”* mediation. With these boundary conditions, we perform a global χ^2 analysis to obtain the parameters consistent with 11 low energy observables, including the top, bottom, and tau masses. Both boundary conditions have universal scalar masses and “just so” splitting for the up- and down-type Higgs masses. In these models, the third family scalars are lighter than the first two families and the gauginos are lighter than all the scalars. We therefore focus on the gluino phenomenology in these models. In particular, we estimate the lowest allowed gluino mass in our models coming from the most recent LHC data and compare these to limits obtained using simplified models. We find that the lower bound on $M_{\tilde{g}}$ in Yukawa-unified SO(10) SUSY GUTs is generically ~ 1.2 TEV at the 1σ level unless there is considerable degeneracy between the gluino and the LSP, in which case the bounds are much weaker. Hence many of our benchmark points are not ruled out by the present LHC data and are still viable models which can be tested at LHC 14.

1 Introduction

Supersymmetric grand unified theories (SUSY GUTs) have the remarkable feature of gauge coupling unification [1–6]. This supplies an experimental clue for weak scale SUSY but does not significantly constrain the sparticle spectrum. It has been observed however that SUSY GUT models which have third family Yukawa coupling unification, such as $\text{SO}(10)$ or $\text{SU}(4)_c \times \text{SU}(2)_L \times \text{SU}(2)_R$, can place considerable constraints on the low energy SUSY spectrum [7–10]. The choice of boundary conditions for the soft terms at the GUT scale determines these constraints and can lead to dramatically different low energy SUSY spectra. Requiring Yukawa unification and obtaining good fits to top, bottom, and tau masses limits the number of viable boundary conditions [8, 11–13]. It is therefore manageable to survey the phenomenological implications for the LHC of viable Yukawa-unified SUSY GUTs. We restrict our studies to two types of $\text{SO}(10)$ boundary conditions: (i) universal gaugino masses and (ii) non-universal gaugino masses with *effective “mirage”* mediation [14]. Both boundary conditions have universal scalar masses and “just so” splitting for the up- and down-type Higgs masses. In these models, the third family scalars are lighter than the first two families [15]. Additionally, the gauginos are lighter than all the scalars. We therefore focus on the gluino phenomenology in these models.

Exclusion limits for the gluino are reported in the context of various Simplified Models by the ATLAS and CMS collaborations. The current exclusion limits on simplified models in which the gluino decays to a pair of third family quarks and the lightest neutralino or chargino are ~ 1.3 TeV at the 1σ level [16, 17]. In Ref. [18], the phenomenological consequences of the Yukawa-unified $\text{SO}(10)$ SUSY GUT with universal gaugino masses were explored using three different sparticle searches performed by the CMS collaboration [19–21]. A lower bound of ~ 1 TeV was found for the gluino mass, which is $\sim 20\%$ below the bound placed by simplified models in the searches considered.¹ The results reported in this paper supersede those reported in Ref. [18]. In addition, we also study the exclusion limits for the gluino in models with non-universal gaugino masses. To complement the CMS searches, we evaluate each of the benchmark models with the code `CheckMATE` [22], which is optimized for simulating many ATLAS searches. We present here the results for the exclusion limits on the gluino mass in the two variants of Yukawa-unified $\text{SO}(10)$ SUSY GUTs.

In Section 2 we present the benchmark models derived for the different boundary conditions considered. The relevant experimental analyses and results are presented in Section 3. We give concluding remarks in Section 4.

2 Benchmark Models

A global χ^2 analysis was performed by varying the GUT scale model parameters, listed in Tab. 1, to fit 11 low energy observables, M_W , M_Z , G_F , α_{em}^{-1} , $\alpha_s(M_Z)$, M_t , $m_b(m_b)$, M_τ , $\mathcal{B}(B \rightarrow X_s \gamma)$, $\mathcal{B}(B_s \rightarrow \mu^+ \mu^-)$, and M_h [13, 14]. Good fits to the low energy observables determined the SUSY spectrum in two scenarios: universal and non-universal gaugino masses. In Ref [13], a full three family model

¹Unfortunately, the branching ratios of the gluino presented in Ref. [18] had an error due to the manner in which our spectrum calculator `maton` was interfaced with `SDECAY` (which calculated the decay branching ratios). The error affected the specific branching ratios reported in Tab. 3 of [18], but the overall results quoted in the paper remain unchanged.

was also considered with an additional D_3 family symmetry and good fits to 36 observables were obtained, but it was shown that the soft SUSY spectrum was completely determined by considering a third family model and fitting the observables listed above. For the purposes of discussing the LHC phenomenology of these models, we will limit the analysis in this paper to the third family model. Note that by good fits we refer to $\chi^2/d.o.f.$ less than 1.0, 2.6, and 3.8 at 68%, 90%, and 95% confidence levels, respectively. The number of degrees of freedom (*d.o.f.*) is defined to be the difference between the number of observables used in the fit and the number of parameters that are allowed to vary in the analysis.

Sector	Universal Gaugino Masses	#	Non-universal Gaugino Masses	#
gauge	$\alpha_G, M_G, \epsilon_3$	3	$\alpha_G, M_G, \epsilon_3$	3
SUSY (GUT scale)	$m_{16}, M_{1/2}, A_0, m_{H_u}, m_{H_d}$	5	$m_{16}, M_{1/2}, \alpha, A_0, m_{H_u}, m_{H_d}$	6
textures	λ	1	λ	1
SUSY (EW scale)	$\tan \beta, \mu$	2	$\tan \beta, \mu$	2
Total #		11		12

Table 1: The $SO(10)$ GUT models with universal and non-universal gaugino masses are both defined by three gauge parameters, $\alpha_G, M_G, \epsilon_3$; one large Yukawa coupling, λ ; μ , and $\tan \beta$ are obtained at the weak scale by consistent electroweak symmetry breaking. There are 5 SUSY parameters defined at the GUT scale: m_{16} (universal scalar mass for squarks and sleptons), $M_{1/2}$ (universal gaugino mass), A_0 (universal trilinear scalar coupling), and m_{H_u}, m_{H_d} (up and down Higgs masses). The models with non-universal gaugino masses have one additional parameter in the SUSY sector, α , which is the ratio of anomaly mediation to gravity mediation contribution to gaugino masses.

2.1 Universal Gaugino Masses

The minimal Yukawa-unified $SO(10)$ SUSY GUT is defined by universal squark and slepton masses, m_{16} , a universal cubic scalar parameter, A_0 , universal gaugino masses, $M_{1/2}$, and non-universal Higgs masses, or “just so” Higgs splitting, m_{H_u}, m_{H_d} or $m_{H_{u(d)}}^2 = m_{10}^2 (1 - (+)\Delta_{m_H}^2)$.² Radiative electroweak symmetry breaking requires $\Delta_{m_H}^2 \approx 13\%$. Furthermore, μ is taken to be positive. Fitting the top, bottom, and tau masses restricts to the region of SUSY breaking parameter space with

$$A_0 \approx -2m_{16}, m_{10} \approx \sqrt{2}m_{16}, m_{16} > \text{few TeV}, \mu, M_{1/2} \ll m_{16}; \quad (1)$$

and, due to Yukawa unification of the third family at the GUT scale,

$$\tan \beta \approx 50. \quad (2)$$

The χ^2 analysis favors a large universal scalar mass, $m_{16} \simeq 20$ TeV [13]. Benchmark points for the universal gaugino mass scenario are shown in Tab. 2. The main features of the low-energy spectrum are as follows. The choice of the soft-terms at the GUT scale results in an inverted scalar mass hierarchy at the weak scale with the first and second generation scalars being much heavier than the third family. The first and second family squarks have masses equal to m_{16} while the third generation squarks are much lighter. Fitting the branching ratio $\mathcal{B}(B_s \rightarrow \mu^+ \mu^-)$ leads to a

² Here, we consider ad hoc splitting between the up- and the down-type Higgs masses. In principle, there can be D-term contributions [11] that can give rise to splitting between the Higgs masses of the form $m_{H_{u(d)}}^2 = m_{10}^2 - (+)2D$. Note that these D-term contributions also give additional splitting to the right- and left-handed scalars.

heavy CP-odd Higgs mass and places us in the decoupling limit. Thus the light Higgs is predicted to be Standard Model-like. The gauginos are much lighter than the scalars and thus the particles in this spectrum that are accessible at the LHC are the gluinos, the lightest neutralino, and the lightest chargino. Furthermore, as shown in Tab. 2, the χ^2 analysis favors lighter gluino masses and the model will be in tension with low energy observables (especially the 125 GeV Higgs mass) if the gluinos are not discovered to be lighter than $\simeq 2$ TeV [13]. The gluino branching ratios of the benchmark points for the universal case are calculated using SDECAY [23] and given in Tab. 3. The dominant branching ratio of the gluino is $\mathcal{B}(\tilde{g} \rightarrow t\bar{b}\tilde{\chi}_1^\pm)$. The remaining contributions to the gluino decays are to $t\bar{t}\tilde{\chi}_i^0$ and $b\bar{b}\tilde{\chi}_i^0$ ($i=1,2$). $\tilde{\chi}_2^0$ is wino-like and relatively light so it plays a role in gluino decays. The lightest neutralino is bino-like and, if the dominant dark matter candidate, would over-close the universe.

Universal	Ua	Ub	Uc	Ud	Ue	Uf
$M_{1/2}$	150	200	250	300	400	600
μ	869	890	824	879	924	974
$\chi^2/\text{d.o.f}$	0.11	0.21	0.38	0.58	1.12	1.98
M_A	2300	2323	2263	2300	2361	2751
$M_{\tilde{g}}$	802	932	1061	1187	1309	1430
$M_{\tilde{t}_1}$	3776	3790	3696	3728	3760	3776
$M_{\tilde{b}_1}$	4634	4654	4580	4608	4640	4628
$M_{\tilde{\tau}_1}$	7865	7886	7834	7861	7896	7890
$M_{\tilde{\chi}_1^0}$	129	151	173	195	217	239
$M_{\tilde{\chi}_2^0}$	264	303	342	382	422	461
$M_{\tilde{\chi}_3^0}$	873	893	828	882	927	977
$M_{\tilde{\chi}_4^0}$	876	897	833	887	932	982
$M_{\tilde{\chi}_1^+}$	264	303	342	382	422	461
$M_{\tilde{\chi}_2^+}$	877	898	833	888	933	982

Table 2: Benchmark points of the universal case with $m_{16} = 20$ TeV. The benchmark points have been chosen with varying values of gluino mass. The model provides good fits to all low-energy observables at 95% C.L.s for $M_{\tilde{g}} < 2000$ GeV [13]. The above fits were obtained by fixing m_{16} and $M_{1/2}$ (to obtain unique gluino masses) and thus yielding 2 d.o.f. for this system.

2.2 Non-universal gaugino masses

Non-universal gaugino masses can be obtained by considering a hybrid SUSY breaking mechanism. In Ref. [14], it was shown that Yukawa unification could be obtained with gravity and anomaly mediation contributions to the gaugino masses [24–27]. The gaugino masses are given by

$$M_i = \left(1 + \frac{g_G^2 b_i \alpha}{16\pi^2} \log \left(\frac{M_{Pl}}{m_{16}} \right) \right) M_{1/2}, \quad (3)$$

Universal	Ua	Ub	Uc	Ud	Ue	Uf
$\mathcal{B}(\tilde{g} \rightarrow g\tilde{\chi}_i^0)$	0%	0%	2%	2%	2%	2%
$\mathcal{B}(\tilde{g} \rightarrow t\tilde{\chi}_1^0)$	6%	7%	7%	7%	8%	8%
$\mathcal{B}(\tilde{g} \rightarrow t\tilde{\chi}_2^0)$	8%	11%	13%	14%	15%	15%
$\mathcal{B}(\tilde{g} \rightarrow b\tilde{\chi}_1^0)$	5%	4%	3%	3%	3%	3%
$\mathcal{B}(\tilde{g} \rightarrow b\tilde{\chi}_2^0)$	18%	16%	14%	13%	12%	11%
$\mathcal{B}(\tilde{g} \rightarrow t\tilde{\chi}_1^\pm)$	62%	62%	60%	60%	58%	56%
$\mathcal{B}(\tilde{g} \rightarrow t\tilde{\chi}_2^\pm)$	0%	0%	0%	0%	2%	2%

Table 3: Gluino decay branching ratios into different final states for the six benchmark models given in Tab. 2. For each model, we give the dominant branching fractions. The loop decays in the first row include all four neutralinos. These ratios were calculated using SDECAY [23].

where $b_i = (33/5, 1, -3)$ for $i = 1, 2, 3$, $M_{1/2}$ is the overall mass scale, and α is the ratio of the anomaly mediation to gravity mediation contributions. The size of α plays a crucial role in determining the ratio of the gaugino masses and in addition the spectrum that is consistent with Yukawa unification. When $\alpha > 4$, the gaugino masses M_1, M_2 and M_3 have opposite signs. We refer to this region of parameter space as “large α ”. For $\alpha < 4$, or “small α ”, the M_i all have the same sign. The relative sign of the gaugino masses leads to qualitatively different low energy spectra. We elaborate below on the benchmark models obtained for various values of α . Note that values of α between 3 and 4 cause the gluino to be the LSP. We do not consider this region. The other soft-terms are similar to the case of universal gaugino masses. There is a universal scalar mass for the squarks and sleptons, m_{16} , a universal cubic scalar parameter, A_0 , and non-universal Higgs mass parameters, m_{H_u} and m_{H_d} . Finally, $\tan \beta \approx 50$.

2.2.1 Small α

When $\alpha < 4$, there are small non-universal contributions to the gaugino masses. The additional degree of freedom, α , allows tuning of the ratios of M_1 and M_2 . As α is gradually increased from 0, there are two effects to the spectrum. The first one is that the wino component of the LSP begins to increase. Therefore, it is possible to obtain the correct relic density by tuning $M_{1/2}$, α , and μ . Secondly, since the beta-function coefficient is negative for SU(3), the gluino mass decreases with increasing α until it becomes the lightest supersymmetric particle for $\alpha \gtrsim 3$. The region in the parameter space that fits the measured value of dark matter relic abundance is of special interest and was studied in Ref. [28] (see also [27, 29, 30]). We show two sample benchmark models which reproduce the measured relic abundance [31] in Tab. 4. Point DMA is well-tempered bino-wino-higgsino mixture whereas point DMb has a bino-wino mixture. The spin independent scattering cross-section for the benchmark point DMA is 1.6×10^{-8} pb. Note that this benchmark point is now ruled out by LUX results [32], which exclude spin independent scattering cross-sections down to 6×10^{-9} pb. An LSP of higher mass can be obtained by increasing the values of $M_{1/2}$ and μ while maintaining the relic density with bino-wino-higgsino well-tempering and be consistent with

Small α	DMa	DMb	COa	COb
ϵ_3	0.00	0.00	0.01	0.01
$M_{1/2}$	450	600	450	485
α	1.5	2.3	2.54	2.61
μ	660	1199	1027	1035
m_{16}	20000	29781	20000	20000
$\chi^2/\text{d.o.f}$	0.92	0.86	1.07	1.19
M_A	1915	3093	2442	3069
$M_{\tilde{g}}$	1130	1135	707	697
$M_{\tilde{t}_1}$	3612	5832	3928	3951
$M_{\tilde{b}_1}$	4770	7543	5453	5431
$M_{\tilde{\tau}_1}$	6867	10565	8026	8024
$M_{\tilde{\chi}_1^0}$	474	799	614	655
$M_{\tilde{\chi}_2^0}$	557	836	629	683
$M_{\tilde{\chi}_3^0}$	663	1201	1030	1038
$M_{\tilde{\chi}_4^0}$	694	1211	1037	1047
$M_{\tilde{\chi}_1^+}$	555	836	615	656
$M_{\tilde{\chi}_2^+}$	691	1210	1037	1045
Ωh^2	0.121	0.099	0.011	0.011

Table 4: Benchmark points for models consistent with Yukawa unification with small non-universal contributions to the gaugino masses. The gaugino spectrum becomes increasingly compressed with increasing α . The well-tempered dark matter points were obtained by fixing μ , $M_{1/2}$ and α to get the right admixture for the LSP. The compressed spectrum points were obtained by fixing m_{16} , $M_{1/2}$, and α to obtain the small splitting between the gluino and the neutralino. There were 2 d.o.f. in determining the best fit points shown above.

the LUX result. On the other hand, the spin independent scattering cross section for point DMb is below the bounds from LUX at 3.5×10^{-9} pb. The dominant decay modes of the gluino for points DMa and DMb are also very similar to the universal case with large decay fractions into the 3-body modes: $t\tilde{b}\tilde{\chi}^\pm$, $t\tilde{t}\tilde{\chi}^0$, $b\tilde{b}\tilde{\chi}^0$.

Another region of interest is when α is slightly less than 3 and the gauginos are nearly degenerate [27, 29]. In this region, the gluino is only a few GeV heavier than the LSP. Sample benchmark points, COa and COb, are presented in Tab. 4. The phenomenology of this region is interesting since the decay products of the gluino will be soft and may not be visible at the LHC. Also, as shown in Tab. 5, the loop decays of the gluino into $g\tilde{\chi}^0$ start dominating over the 3-body decays. The LSP contains a large wino component and the relic abundance is not saturated for these values of α .

The best fit points obtained with $\alpha < 4$ are very similar to the benchmark points discussed in the case of universal gaugino masses. The first two family of scalars are very heavy ($\sim m_{16}$), and the spectrum has the inverted scalar mass hierarchy. The extra MSSM Higgses are heavy and decoupled

Small α	DMa	DMb	COa	COb
$BR(\tilde{g} \rightarrow g\tilde{\chi}_1^0)$	0%	2%	41%	83%
$BR(\tilde{g} \rightarrow g\tilde{\chi}_2^0)$	1%	2%	3%	1%
$BR(\tilde{g} \rightarrow g\tilde{\chi}_3^0)$	6%	0%	0%	0%
$BR(\tilde{g} \rightarrow g\tilde{\chi}_4^0)$	4%	0%	0%	0%
$BR(\tilde{g} \rightarrow t\bar{t}\tilde{\chi}_1^0)$	2%	0%	0%	0%
$BR(\tilde{g} \rightarrow t\bar{t}\tilde{\chi}_2^0)$	4%	0%	0%	0%
$BR(\tilde{g} \rightarrow t\bar{t}\tilde{\chi}_3^0)$	4%	0%	0%	0%
$BR(\tilde{g} \rightarrow t\bar{t}\tilde{\chi}_4^0)$	3%	0%	0%	0%
$BR(\tilde{g} \rightarrow b\bar{b}\tilde{\chi}_1^0)$	4%	14%	51%	15%
$BR(\tilde{g} \rightarrow b\bar{b}\tilde{\chi}_2^0)$	9%	38%	2%	0%
$BR(\tilde{g} \rightarrow b\bar{b}\tilde{\chi}_3^0)$	7%	0%	0%	0%
$BR(\tilde{g} \rightarrow b\bar{b}\tilde{\chi}_4^0)$	4%	0%	0%	0%
$BR(\tilde{g} \rightarrow t\bar{b}\tilde{\chi}_1^\pm)$	32%	42%	0%	0%
$BR(\tilde{g} \rightarrow t\bar{b}\tilde{\chi}_2^\pm)$	20%	0%	0%	0%

Table 5: Gluino decay branching ratios into different final states for the DM (dark matter) and CO (compressed gaugino spectrum) benchmark models given in Tab. 4. For each model, we give the dominant branching fractions. These ratios were calculated using SDECAY [23].

and thus the lightest Higgs is purely SM like. The benchmark points prefer the value of $\epsilon_3 \approx 0 - 1\%$. ϵ_3 is the GUT scale threshold correction required to fit the value of $\alpha_s(M_Z)$. While standard MSSM scenarios with universal gaugino mass prefer $\epsilon_3 = -3\%$, it was shown in Ref. [30, 33] that precision gauge coupling unification can be achieved in models with non-universal gaugino masses, especially with the mirage pattern with lighter gluinos considered in this work.

2.2.2 Large α

For $\alpha > 4$, M_1 and M_2 have the opposite sign as M_3 . We choose $\mu, M_{1/2} < 0$ and thus fix $M_3 > 0$, $M_1, M_2 < 0$. The first and second family squarks and sleptons have mass of order $m_{16} = 5$ TeV while the third family scalars are roughly a factor of 2 lighter. In addition, gluinos are always lighter than the third family squarks and sleptons, and the lightest charginos and neutralinos are even lighter. The third generation squarks have mass ~ 1.6 TeV and the lightest neutralino and the lightest chargino are nearly degenerate. The LSP is wino-like and, if the dominant thermal dark matter component, produces an under-abundant dark matter relic. Since the chargino and neutralino are nearly degenerate, 1-loop corrections to the mass difference has been estimated based on Ref. [34]. If the mass difference is less than $\simeq 1.5$ GeV, then the charginos decay to the neutralino and pions. These decay widths have also been calculated using Ref. [35].

The particles in the spectrum that are accessible at the LHC are the gluinos, the two lightest neutralinos, and the lightest chargino. In contrast to the universal case, the χ^2 analysis does not favor any specific range of gluino masses (cf. Tab. 6). The masses and gluino branching ratios of the

benchmark points for the large α case are given in Tab. 6 and Tab. 7, respectively. The dominant branching ratio of the gluino is $\mathcal{B}(\tilde{g} \rightarrow t\bar{t}\tilde{\chi}_i^\pm)$ ($i=1,2$). The remaining contributions to the gluino decays are to $t\bar{t}\tilde{\chi}_j^0$ and $b\bar{b}\tilde{\chi}_j^0$ ($j=1,2,3$). The neutralinos are more degenerate so the heavier ones contribute a non-negligible amount to the branching ratios.

Large α	Ma	Mb	Mc	Md	Me	Mf
$M_{1/2}$	-181	-200	-220	-200	-200	-200
μ	-341	-341	-346	-355	-376	-405
α	6	8	8	9	10	11
$\chi^2/\text{d.o.f.}$	0.36	0.40	0.45	0.41	0.41	0.42
M_A	2549	2513	2490	2510	2453	2383
$M_{\tilde{g}}$	859	940	1025	1107	1270	1429
$M_{\tilde{t}_1}$	1717	1734	1764	1799	1864	1937
$M_{\tilde{b}_1}$	1490	1522	1561	1592	1680	1780
$M_{\tilde{\tau}_1}$	2132	2124	2126	2128	2131	2148
$M_{\tilde{\chi}_1^0}$	276	290	305	307	327	352
$M_{\tilde{\chi}_2^0}$	347	346	351	360	381	409
$M_{\tilde{\chi}_3^0}$	389	405	428	423	443	467
$M_{\tilde{\chi}_4^0}$	576	632	693	698	764	830
$M_{\tilde{\chi}_1^+}$	279	294	309	310	331	355
$M_{\tilde{\chi}_2^+}$	395	409	431	426	447	470

Table 6: Benchmark points of the mirage case with $m_{16} = 5$ TeV. The gaugino sector of the model is different from the universal case, good fits are obtained for heavier gluino masses and the lightest chargino and neutralino are nearly degenerate. In addition to m_{16} , $M_{1/2}$ and α were also held fixed in order to obtain unique values of the gluino mass.

3 Experimental Analyses and Results

The searches for new physics by the ATLAS and CMS collaborations are often interpreted within the context of simplified models. Such models are intended to capture the main features of specific scenarios with the risk being that the assumptions are over-simplified. The simplified models studied by the collaborations that most resemble our models assume branching ratios of $\mathcal{B}(\tilde{g} \rightarrow t\bar{t}\tilde{\chi}_1^0) = 100\%$, $\mathcal{B}(\tilde{g} \rightarrow b\bar{b}\tilde{\chi}_1^0) = 100\%$, or $\mathcal{B}(\tilde{g} \rightarrow t\bar{t}\tilde{\chi}_1^\pm) = 100\%$. However, the branching ratios for our models clearly do not match the decay branching ratio for any one simplified model. Fortunately, the ATLAS and CMS collaborations provide, for a given search and signal region therein, an allowed number of events from new physics. It is thus possible to reinterpret the searches for new physics in the context of more elaborate models. The contribution of a sparticle to the number of events in a signal region is a function of the production cross section of the sparticle and the sparticle's branching fraction into final states relevant to the signal region. By comparing this contribution to

Large α	Ma	Mb	Mc	Md	Me	Mf
$\mathcal{B}(\tilde{g} \rightarrow g\tilde{\chi}_1^0)$	0%	0%	0%	0%	0%	0%
$\mathcal{B}(\tilde{g} \rightarrow g\tilde{\chi}_2^0)$	2%	1%	1%	1%	1%	0%
$\mathcal{B}(\tilde{g} \rightarrow g\tilde{\chi}_3^0)$	1%	0%	0%	0%	0%	0%
$\mathcal{B}(\tilde{g} \rightarrow g\tilde{\chi}_4^0)$	0%	0%	0%	0%	0%	0%
$\mathcal{B}(\tilde{g} \rightarrow t\tilde{\chi}_1^0)$	7%	8%	9%	8%	9%	9%
$\mathcal{B}(\tilde{g} \rightarrow t\tilde{\chi}_2^0)$	4%	6%	7%	8%	8%	9%
$\mathcal{B}(\tilde{g} \rightarrow t\tilde{\chi}_3^0)$	1%	1%	1%	1%	2%	3%
$\mathcal{B}(\tilde{g} \rightarrow t\tilde{\chi}_4^0)$	0%	0%	0%	0%	0%	0%
$\mathcal{B}(\tilde{g} \rightarrow b\tilde{\chi}_1^0)$	19%	16%	15%	14%	12%	11%
$\mathcal{B}(\tilde{g} \rightarrow b\tilde{\chi}_2^0)$	13%	13%	12%	12%	11%	11%
$\mathcal{B}(\tilde{g} \rightarrow b\tilde{\chi}_3^0)$	7%	6%	6%	6%	6%	6%
$\mathcal{B}(\tilde{g} \rightarrow b\tilde{\chi}_4^0)$	0%	0%	0%	0%	0%	0%
$\mathcal{B}(\tilde{g} \rightarrow t\tilde{\chi}_1^\pm)$	30%	32%	36%	32%	32%	32%
$\mathcal{B}(\tilde{g} \rightarrow t\tilde{\chi}_2^\pm)$	16%	14%	12%	16%	18%	20%

Table 7: Gluino decay branching ratios into different final states for the eight benchmark models given in Tab. 6. For each model, we give the dominant branching fractions. These ratios were calculated using SDECAY [23].

the allowed number of events from new physics, an exclusion limit can be set on the sparticle’s mass. For both boundary conditions considered in this paper, the squarks and sleptons are sufficiently heavier than the gauginos and thus do not contribute to the final states relevant for gluino or electroweakino³ searches. Furthermore, searches designed to look for gluinos do not overlap with those designed to look for electroweakinos. That is, electroweakinos do not contribute to signal regions from searches for gluinos, and vice versa. This is at least true for our models. Since there is no contamination from other sparticles, we are able to directly place bounds on the gluino masses in our models.

The procedure of Ref. [18] was performed for each benchmark model considered here to determine the limits from the 3 CMS analyses. In addition, the program CheckMATE⁴ was used to evaluate bounds on the gluino mass for each model. CheckMATE requires as input a HepMC [40] file containing generated events and the production cross section of the sparticles of interest along with the total 1σ uncertainty on the cross section. We use PYTHIA 8.175 [41] to generate 10,000–20,000 events in HepMC format.⁵ The gluino production cross section and its uncertainty are obtained from [42]. It was found that the ATLAS analysis ATLAS-CONF-2013-061 [16], on which we elaborate below, is the most constraining analysis for each of the benchmark points in our models with the exception of COa and COb. These two points were not ruled out by any analysis considered in this paper. The analysis which came the closest to ruling out these points was the ATLAS analysis ATLAS-CONF-2013-047 [43], which is a search for final states with high- p_T jets, missing transverse momentum,

³Electroweakinos refer to neutralinos and charginos, collectively.

⁴CheckMATE uses Delphes 3 [36], FastJet [37, 38], and the Anti-kt jet algorithm [39].

⁵We are using HepMC 2.06.09.

and no electrons or muons. Both of these analyses are implemented in `CheckMATE`.

The ATLAS-CONF-2013-061 analysis is a search for final states with large missing transverse momentum, at least four, six, or seven jets, at least three jets tagged as b -jets, and either zero or at least one lepton. It was performed at $\sqrt{s} = 8$ TeV with 20.1 fb^{-1} of data. The results are interpreted in the context of a variety of simplified models. The simplified models considered that are relevant to our models are the Gbb, Gtt, and Gtb models. These models assume 100% branching ratios of a gluino to $b\bar{b}\tilde{\chi}_1^0$, $t\bar{t}\tilde{\chi}_1^0$, and $t\tilde{b}\tilde{\chi}_1^\pm$, respectively. The most constraining signal regions on our models are presented in Tab. 8 for the universal and dark matter cases and in Tab. 9 for the large α case. The universal and dark matter cases are constrained most by the signal region requiring at least 1 lepton and at least 6 jets while the large α case is most constrained by the signal region requiring no leptons and at least 4 jets. Each of the benchmark points in these cases has a sizeable gluino branching fraction into $t\tilde{b}\tilde{\chi}_1^\pm$. For the universal and dark matter points, the mass splitting of the lightest chargino and the lightest neutralino is large enough for the chargino to decay to a W whose decay products are energetic enough to be seen in the detector. This is not true for the large α case. The lightest chargino and the lightest neutralino in the large α benchmark points are nearly degenerate and so the charginos produced from gluino decays in these points are effectively missing energy.

baseline selection: ≥ 1 signal lepton (e, μ), $p_T^{j_1} > 90 \text{ GeV}$, $E_T^{\text{miss}} > 150 \text{ GeV}$, ≥ 4 jets with $p_T > 30 \text{ GeV}$, ≥ 3 b -jets with $p_T > 30 \text{ GeV}$					
Signal Region	N jets	E_T^{miss} [GeV]	m_T [GeV]	$m_{\text{eff}}^{\text{incl}}$ [GeV]	$E_T^{\text{miss}} / \sqrt{H_T^{\text{incl}}}$ [$\text{GeV}^{\frac{1}{2}}$]
SR-11-6J-B	≥ 6	> 225	> 140	> 800	> 5

Table 8: Most constraining signal region for the universal and dark matter scenarios. A detailed description of the parameters in this table can be found in [16].

baseline selection: baseline lepton veto, $p_T^{j_1} > 90 \text{ GeV}$, $E_T^{\text{miss}} > 150 \text{ GeV}$, ≥ 4 jets with $p_T > 30 \text{ GeV}$, $\Delta\phi_{\text{min}}^{4j} \geq 0.5$, $E_T^{\text{miss}}/m_{\text{eff}}^{4j} > 0.2$, ≥ 3 b -jets with $p_T > 30 \text{ GeV}$				
Signal Region	N jets	E_T^{miss} [GeV]	p_T jets [GeV]	m_{eff}^{4j} [GeV]
SR-01-4J-C	≥ 4	> 250	> 50	> 1300

Table 9: Most constraining signal region for the large α scenario. A detailed description of the parameters in this table can be found in [16].

In the ATLAS analysis, the number of observed events in a given signal region is used to calculate a 95% confidence level (CL) upper limit on the allowed number of events by new physics. Each of the simplified models (Gbb,Gtt,Gtb) has two free parameters: the gluino mass and the neutralino

mass.⁶ These two parameters are scanned over for a simplified model and a predicted number of events for the various signal regions is calculated. By comparing the predicted number to the 95% CL upper limit, an observed limit is found in the gluino-neutralino masses parameter space with $\pm 1\sigma$ theoretical uncertainty. In **CheckMATE**, the number of signal events S is determined for each signal region of a given analysis. The total 1σ uncertainty on this number ΔS is calculated from both the statistical uncertainty, given by Monte Carlo generated events, and the systematic uncertainty, which is estimated from the total uncertainty on the signal cross section provided by the user. In order to compare results from **CheckMATE** to those in the ATLAS analysis, we calculate the ratio r of the predicted number of signal events at the 1σ theoretical lower limit to the experimentally measured 95% CL upper limit provided by the ATLAS analysis,⁷

$$r \equiv \frac{S - \Delta S}{S_{\text{Exp}}^{95}} . \quad (4)$$

A model is considered excluded if this ratio is ≥ 1 . As a check, we calculate the bounds for the simplified models (Gbb,Gtt,Gtb) and obtain good agreement with the results of the ATLAS analysis (cf. Fig. 12 and Fig. 14 in [16]).⁸ We then obtain exclusion limits on the gluino mass in our models. Points Ua-d are ruled out for the universal case and points Ma-d are ruled out for the large α case. In the dark matter scenario, the point DMA is ruled out while the point DMb is allowed. Point DMb is not well-constrained due to the small mass differences between the gluino and the lightest electroweakinos, $\Delta m_{\tilde{g}-\tilde{\chi}} \approx 300$ GeV (cf. Tab. 4).

There are 6 dominant branching ratios in our models: $b\bar{b}\tilde{\chi}_1^0$, $t\bar{t}\tilde{\chi}_1^0$, $t\bar{b}\tilde{\chi}_1^\pm$, $b\bar{b}\tilde{\chi}_2^0$, $t\bar{t}\tilde{\chi}_2^0$, and $t\bar{b}\tilde{\chi}_2^\pm$. We find that the bounds for simplified models defined by 100% branching fractions to $b\bar{b}\tilde{\chi}_1^0$, $t\bar{t}\tilde{\chi}_1^0$, or $t\bar{b}\tilde{\chi}_1^\pm$ are approximately equal. We also find that simplified models defined by 100% branching fractions to $t\bar{t}\tilde{\chi}_2^0$ and $t\bar{b}\tilde{\chi}_2^\pm$ receive nearly the same limits. We can therefore represent our models to a good approximation by models with branching fractions to combinations of $t\bar{b}\tilde{\chi}_1^\pm$, $b\bar{b}\tilde{\chi}_2^0$, and $t\bar{t}\tilde{\chi}_2^0$. As a complementary approach to testing the benchmark points directly and to obtain a more general representation of the bounds on models such as ours, we obtain exclusion limits for models defined by branching fractions to all combinations of these three decay modes and record the bounds on a triangle [44] as shown in Fig. 1. This approach is particularly useful for testing an approximately continuous range of gluino masses when the benchmark points have large differences between their gluino masses, as is the case for the universal and large α scenarios. While the range of exclusion limits shown in Fig. 1 spans ~ 100 GeV, it is clear that the ATLAS search ATLAS-CONF-2013-061 is sensitive to all six of the third-family-mediated gluino decay modes listed above.

In the universal case, each of the benchmark models shares nearly the same combination of branching ratios and can therefore be represented by a single point on the triangle. We represent this case by the black star in Fig. 1. This observation is also true for the large α case which we represent by a red dot. Note that the decay modes considered in the triangle only constitute $\sim 90\%$ of the branching ratios for models in the large α case. It is still useful however to see where these models lie in the triangle so that a comparison can be drawn with the universal case. These two cases

⁶In the Gtb model, the mass difference between the chargino and neutralino is set to 2 GeV. So, there are still only two free parameters in this model.

⁷Note that by default **CheckMATE** calculates r at the 2σ theoretical lower limit.

⁸We consider only individual signal regions when testing models and therefore compare our results to those in the ATLAS analysis coming from individual signal regions.

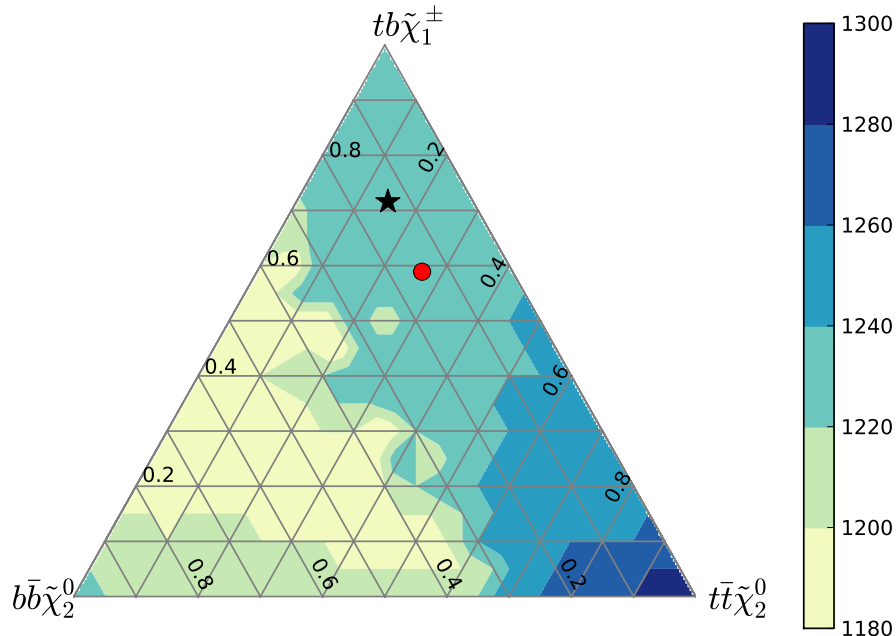


Figure 1: Lowest gluino masses allowed by Ref. [16] for models with branching fractions to combinations of $tb\tilde{\chi}_1^\pm$, $b\bar{b}\tilde{\chi}_2^0$, and $t\bar{t}\tilde{\chi}_2^0$. All masses are in GeV. The black star and red dot are representative points for the universal and large α cases, respectively. We set $M_{\tilde{\chi}_1^0} = 200$ GeV and $M_{\tilde{\chi}_2^0} = 300$ GeV for the generation of these points.

inhabit the same region of the triangle and thus both have exclusion limits on the gluino mass of ~ 1.2 TeV. This is consistent with the limits obtained by testing the benchmark points directly.

The exclusion limits on the mass of the gluino obtained for the benchmark models at the 1σ level are summarized in Fig. 2. They are arranged with increasing α with the universal case corresponding to $\alpha = 0$. Each model scenario in the plot is color coded with its main features listed in the box below the plot with corresponding color. Models in regions with diagonal slashes have been ruled out by the ATLAS search ATLAS-CONF-2013-061. Vertical black lines denote the region in which the benchmark points COa and COb have exclusion limits.⁹ The horizontal lines show the region in α -space where models have a gluino LSP, which we did not consider in this paper. We find that the lower bound on $M_{\tilde{g}}$ in Yukawa-unified SO(10) SUSY GUTs is generically ~ 1.2 TeV at the 1σ level unless there is considerable degeneracy between the gluino and the LSP, in which case the bounds are much lower.

4 Conclusion

In this paper, we surveyed the LHC phenomenology of Yukawa-unified SO(10) SUSY GUTs with various GUT scale boundary conditions. These boundary conditions are characterized by (i) univer-

⁹ The current bound on the gluino mass in such scenarios is ~ 550 GeV [43, 45].

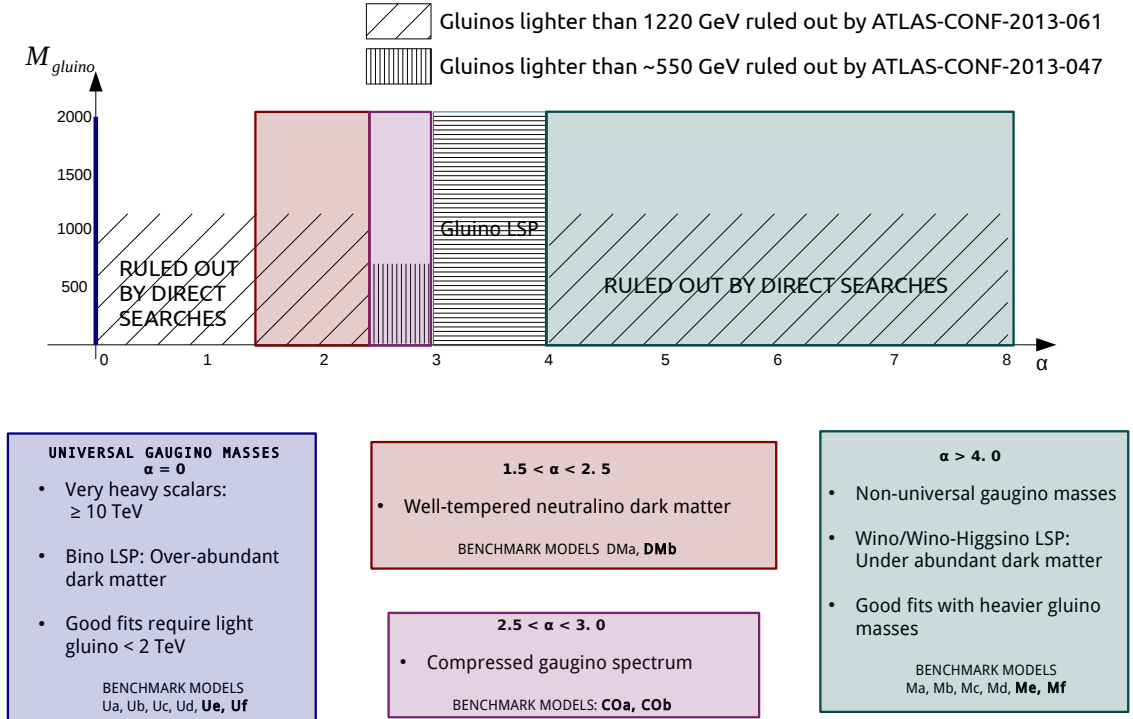


Figure 2: Summary of the exclusion limits obtained for the benchmark models considered in this paper. The main features of each model scenario are listed in the boxes below the plot. Benchmark points listed in bold are not ruled out.

sal scalar masses and universal gaugino masses or by (ii) universal scalar masses and non-universal gaugino masses with effective mirage mediation. The size of the effective mirage mediation parameter, α , plays a crucial role in determining the ratio of the gaugino masses and in addition the spectrum that is consistent with Yukawa unification. For boundary condition (ii), we considered three scenarios: (ii.1) roughly equal gravity mediated and anomaly mediated contributions to gaugino masses, (ii.2) well-tempered dark matter, and (ii.3) compressed gauginos. A global χ^2 analysis was performed by varying GUT scale model parameters to fit low energy observables. Benchmark points were chosen based on the best fit of the Yukawa-unified SO(10) SUSY GUT models to low-energy data. The particles in the spectra of these models that are accessible at the LHC are the gluinos and the lightest electroweakinos. The focus of this paper was restricted to gluino phenomenology. The gluinos in models (i), (ii.1), and (ii.2) have large decay fractions into the 3-body modes, $tb\tilde{\chi}^\pm$, $t\bar{t}\tilde{\chi}^0$, and $b\bar{b}\tilde{\chi}^0$, while the branching fractions of the gluinos in model (ii.3) into $g\tilde{\chi}^0$ are significant if not dominant.

Using recent experimental analyses relevant to gluino production at the LHC, we derived a lower bound on the gluino mass for each boundary condition except for (ii.3). Model (ii.3) was not constrained by any analysis considered. In this model, the gluino and the LSP are nearly degenerate

so that the gluino decay products are too soft to be seen in the detector. We found that the lower bound on $M_{\tilde{g}}$ in Yukawa-unified SO(10) SUSY GUTs is generically ~ 1.2 TEV at the 1σ level unless there is considerable degeneracy between the gluino and the LSP, in which case the bounds are much lower (cf. footnote 9). Hence many of our benchmark points (cf. Tab. 2, Tab. 4, Tab. 6) are not ruled out by the present LHC data and are still viable models which can be tested at LHC 14. Finally, we note that current exclusion limits on simplified models in which the gluino decays to a pair of third family quarks and the lightest neutralino or chargino are ~ 1.3 TeV at the 1σ level [16, 17].

Acknowledgments

We thank the authors of SDECAY for useful discussions. B.C.B. and S.R. received partial support for this work from DOE/ER/01545-902. A.A. is supported on the Ohio State University Presidential Fellowship. We thank the *Ohio Supercomputer Center* for their computing resources.

References

- [1] S. Dimopoulos, S. Raby, and F. Wilczek, “Supersymmetry and the Scale of Unification,” *Phys.Rev.* **D24** (1981) 1681–1683.
- [2] S. Dimopoulos and H. Georgi, “Softly Broken Supersymmetry and SU(5),” *Nucl.Phys.* **B193** (1981) 150.
- [3] L. E. Ibanez and G. G. Ross, “Low-Energy Predictions in Supersymmetric Grand Unified Theories,” *Phys.Lett.* **B105** (1981) 439.
- [4] N. Sakai, “Naturalness in Supersymmetric Guts,” *Z.Phys.* **C11** (1981) 153.
- [5] M. Einhorn and D. Jones, “The Weak Mixing Angle and Unification Mass in Supersymmetric SU(5),” *Nucl.Phys.* **B196** (1982) 475.
- [6] W. J. Marciano and G. Senjanovic, “Predictions of Supersymmetric Grand Unified Theories,” *Phys.Rev.* **D25** (1982) 3092.
- [7] T. Blazek, R. Dermisek, and S. Raby, “Predictions for Higgs and supersymmetry spectra from SO(10) Yukawa unification with $\mu > 0$,” *Phys.Rev.Lett.* **88** (2002) 111804, [hep-ph/0107097](#).
- [8] T. Blazek, R. Dermisek, and S. Raby, “Yukawa unification in SO(10),” *Phys.Rev.* **D65** (2002) 115004, [hep-ph/0201081](#).
- [9] H. Baer and J. Ferrandis, “Supersymmetric SO(10) GUT models with Yukawa unification and a positive μ term,” *Phys.Rev.Lett.* **87** (2001) 211803, [hep-ph/0106352](#).
- [10] K. Tobe and J. D. Wells, “Revisiting top bottom tau Yukawa unification in supersymmetric grand unified theories,” *Nucl.Phys.* **B663** (2003) 123–140, [hep-ph/0301015](#).
- [11] H. Baer, S. Kraml, and S. Sekmen, “Is ‘just-so’ Higgs splitting needed for t - b - tau Yukawa unified SUSY GUTs?,” *JHEP* **0909** (2009) 005, [0908.0134](#).

- [12] M. Badziak, M. Olechowski, and S. Pokorski, “Yukawa unification in SO(10) with light sparticle spectrum,” *JHEP* **1108** (2011) 147, [1107.2764](#).
- [13] A. Anandakrishnan, S. Raby, and A. Wingerter, “Yukawa Unification Predictions for the LHC,” *Phys.Rev.* **D87** (2013) 055005, [1212.0542](#).
- [14] A. Anandakrishnan and S. Raby, “Yukawa Unification Predictions with effective ”Mirage” Mediation,” *Phys.Rev.Lett.* **111** (2013) 211801, [1303.5125](#).
- [15] D. M. Pierce, J. A. Bagger, K. T. Matchev, and R.-j. Zhang, “Precision corrections in the minimal supersymmetric standard model,” *Nucl.Phys.* **B491** (1997) 3–67, [hep-ph/9606211](#).
- [16] “Search for strong production of supersymmetric particles in final states with missing transverse momentum and at least three b-jets using 20.1 fb1 of pp collisions at $\sqrt{s} = 8$ TeV with the ATLAS Detector.,” Tech. Rep. ATLAS-CONF-2013-061, CERN, Geneva, Jun, 2013.
- [17] **CMS Collaboration** Collaboration, “Search for supersymmetry using razor variables in events with b-jets in pp collisions at 8 TeV,” Tech. Rep. CMS-PAS-SUS-13-004, CERN, Geneva, 2013.
- [18] A. Anandakrishnan, B. C. Bryant, S. Raby, and A. Wingerter, “LHC Phenomenology of SO(10) Models with Yukawa Unification,” *Phys.Rev.* **D88** (2013) 075002, [1307.7723](#).
- [19] **CMS Collaboration** Collaboration, S. Chatrchyan *et al.*, “Search for gluino mediated bottom- and top-squark production in multijet final states in pp collisions at 8 TeV,” [1305.2390](#).
- [20] **CMS Collaboration** Collaboration, S. Chatrchyan *et al.*, “Search for new physics in events with same-sign dileptons and b jets in pp collisions at $\sqrt{s} = 8$ TeV,” *JHEP* **1303** (2013) 037, [1212.6194](#).
- [21] **CMS Collaboration** Collaboration, S. Chatrchyan *et al.*, “Search for supersymmetry in hadronic final states with missing transverse energy using the variables α_T and b-quark multiplicity in pp collisions at $\sqrt{s} = 8$ TeV,” [1303.2985](#).
- [22] M. Drees, H. Dreiner, D. Schmeier, J. Tattersall, and J. S. Kim, “CheckMATE: Confronting your Favourite New Physics Model with LHC Data,” [1312.2591](#).
- [23] M. Muhlleitner, A. Djouadi, and Y. Mambrini, “SDECAY: A Fortran code for the decays of the supersymmetric particles in the MSSM,” *Comput.Phys.Commun.* **168** (2005) 46–70, [hep-ph/0311167](#).
- [24] K. Choi, A. Falkowski, H. P. Nilles, and M. Olechowski, “Soft supersymmetry breaking in KKLT flux compactification,” *Nucl.Phys.* **B718** (2005) 113–133, [hep-th/0503216](#).
- [25] K. Choi, K. S. Jeong, T. Kobayashi, and K.-i. Okumura, “Little SUSY hierarchy in mixed modulus-anomaly mediation,” *Phys.Lett.* **B633** (2006) 355–361, [hep-ph/0508029](#).
- [26] R. Kitano and Y. Nomura, “A Solution to the supersymmetric fine-tuning problem within the MSSM,” *Phys.Lett.* **B631** (2005) 58–67, [hep-ph/0509039](#).

- [27] V. Lowen and H. P. Nilles, “Mirage Pattern from the Heterotic String,” *Phys.Rev.* **D77** (2008) 106007, [0802.1137](#).
- [28] A. Anandakrishnan and K. Sinha, “On the Viability of Thermal Well-Tempered Dark Matter in SUSY GUTs,” [1310.7579](#).
- [29] K. Choi, K. S. Jeong, and K.-i. Okumura, “Phenomenology of mixed modulus-anomaly mediation in fluxed string compactifications and brane models,” *JHEP* **0509** (2005) 039, [hep-ph/0504037](#).
- [30] S. Krippendorf, H. P. Nilles, M. Ratz, and M. W. Winkler, “Hidden SUSY from precision gauge unification,” *Phys.Rev.* **D88** (2013) 035022, [1306.0574](#).
- [31] **Planck Collaboration** Collaboration, P. Ade *et al.*, “Planck 2013 results. I. Overview of products and scientific results,” [1303.5062](#).
- [32] **LUX Collaboration** Collaboration, D. Akerib *et al.*, “First results from the LUX dark matter experiment at the Sanford Underground Research Facility,” [1310.8214](#).
- [33] S. Raby, M. Ratz, and K. Schmidt-Hoberg, “Precision gauge unification in the MSSM,” *Phys.Lett.* **B687** (2010) 342–348, [0911.4249](#).
- [34] H.-C. Cheng, B. A. Dobrescu, and K. T. Matchev, “Generic and chiral extensions of the supersymmetric standard model,” *Nucl.Phys.* **B543** (1999) 47–72, [hep-ph/9811316](#).
- [35] C. Chen, M. Drees, and J. Gunion, “A Nonstandard string / SUSY scenario and its phenomenological implications,” *Phys.Rev.* **D55** (1997) 330–347, [hep-ph/9607421](#).
- [36] **DELPHES 3** Collaboration, J. de Favereau *et al.*, “DELPHES 3, A modular framework for fast simulation of a generic collider experiment,” *JHEP* **1402** (2014) 057, [1307.6346](#).
- [37] M. Cacciari, G. P. Salam, and G. Soyez, “FastJet User Manual,” *Eur.Phys.J.* **C72** (2012) 1896, [1111.6097](#).
- [38] M. Cacciari and G. P. Salam, “Dispelling the N^3 myth for the k_t jet-finder,” *Phys.Lett.* **B641** (2006) 57–61, [hep-ph/0512210](#).
- [39] M. Cacciari, G. P. Salam, and G. Soyez, “The Anti- $k(t)$ jet clustering algorithm,” *JHEP* **0804** (2008) 063, [0802.1189](#).
- [40] M. Dobbs and J. B. Hansen, “The HepMC C++ Monte Carlo event record for High Energy Physics,” *Comput.Phys.Commun.* **134** (2001) 41–46.
- [41] T. Sjostrand, S. Mrenna, and P. Z. Skands, “A Brief Introduction to PYTHIA 8.1,” *Comput.Phys.Commun.* **178** (2008) 852–867, [0710.3820](#).
- [42] M. Kramer, A. Kulesza, R. van der Leeuw, M. Mangano, S. Padhi, *et al.*, “Supersymmetry production cross sections in pp collisions at $\sqrt{s} = 7$ TeV,” [1206.2892](#).
- [43] **ATLAS** Collaboration, “Search for squarks and gluinos with the atlas detector in final states with jets and missing transverse momentum and 20.3 fb $^{-1}$ of $\sqrt{s} = 8$ tev proton-proton collision data.” <http://cds.cern.ch/record/1547563/files/ATLAS-CONF-2013-047.pdf>, May, 2013. ATLAS-CONF-2013-047.

- [44] A. Anandakrishnan and C. S. Hill, “Beyond Simplified Models: Constraining Supersymmetry on Triangles,” [1403.4294](#).
- [45] **CMS Collaboration** Collaboration, S. Chatrchyan *et al.*, “Search for new physics in the multijet and missing transverse momentum final state in proton-proton collisions at $\sqrt{s} = 8$ TeV,” [1402.4770](#).